

Chem Soc Rev

This article was published as part of the
Hybrid materials themed issue

Guest editors Clément Sanchez, Kenneth J. Shea and Susumu Kitagawa

Please take a look at the issue 2 2011 [table of contents](#) to
access other reviews in this themed issue



Cite this: *Chem. Soc. Rev.*, 2011, **40**, 640–655

www.rsc.org/csr

TUTORIAL REVIEW

One-dimensional magnetic inorganic–organic hybrid nanomaterials†

Jiayin Yuan,^a Youyong Xu^b and Axel H. E. Müller^{*c}

Received 19th August 2010

DOI: 10.1039/c0cs00087f

One-dimensional (1D) magnetic inorganic–organic hybrid nanomaterials bear both the intrinsic magnetic properties of the inorganic components and the functionality and responsiveness of their organic part. In this *tutorial review*, we first emphasize various synthetic strategies for this type of materials: (i) template-directed synthesis employs different preformed templates such as channels in solids, mesostructures self-assembled from block copolymers, cylindrical polymer brushes, 1D biological templates and other existing 1D templates; (ii) electrospinning, which provides a simple and efficient technique that can lead to a potential large-scale production; (iii) 1D conjugation of building blocks which combines the physical attraction of magnetic nanoparticles in a magnetic field with chemical crosslinking and stabilization. The properties, functions and the future trends of these materials are also briefly introduced. It is foreseeable that these hybrid materials will play more and more important roles in the ever-advancing miniaturization of functional devices.

1. Introduction

One-dimensional (1D) nanostructures have been intensively studied in the past decades, owing to their unique shape, properties, and applications in nanodevices. However, most of the studies focused on 1D conducting and semiconducting nanomaterials, mainly for the application in microelectronics. Recently, much attention has been paid to 1D magnetic nanomaterials due to their charming and unique properties.

Compared to their spherical counterparts, they show characteristic magnetization features such as coercive force, remanence, and a hysteresis shape, which become anisotropic. Besides the anisotropic nature of the individual, the elongated shape in addition provides preferential mutual interactions when they are organized or assembled, thus the collective behavior as well as physical properties turn anisotropic and vary at different directions. They are of huge interest for use in high density data storage systems, sensing, spintronic devices, and micro/nano-magnetomechanical systems. When coupled with organic functions in a 1D manner, they exhibit some advantages over their single components.

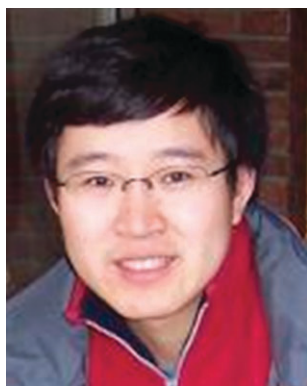
Some inorganic materials, like metals, alloys and metal oxides of Fe, Co or Ni, are responsive to external magnetic fields arising from the aligned interactions of unpaired electron spins of atoms in a crystalline lattice. The term magnetism is used to describe how materials respond on the microscopic

^a Max-Planck-Institut für Kolloid- und Grenzflächenforschung, D-14476 Potsdam, Germany

^b Department of Materials Science and Engineering, Cornell University, Ithaca, NY 14853, USA

^c Makromolekulare Chemie II and Bayreuther Zentrum für Kolloid- und Grenzflächenforschung, Universität Bayreuth, D-95440, Bayreuth, Germany. E-mail: axel.mueller@uni-bayreuth.de; Fax: +49 921-553393; Tel: +49 921-553399

† Part of the themed issue on hybrid materials.



Jiayin Yuan

Jiayin Yuan studied chemistry at the Shanghai Jiao Tong University, China, and the University of Siegen, Germany. In 2009, he received his PhD under the supervision of Prof Axel H. E. Müller at the University of Bayreuth, Germany. Currently, he holds a post-doctoral scholarship in the Max Planck Institute of Colloids and Interfaces in Potsdam, Germany, working with Prof Markus Antonietti.



Youyong Xu

Youyong Xu received his MSc degree in Materials from Shanghai Jiao Tong University, 2004. In 2008, he received his PhD under the supervision of Prof Axel H. E. Müller at the University of Bayreuth, Germany. Currently, he is a postdoctoral associate in Prof Christopher K. Ober's group at Cornell University, Ithaca, NY, USA.

level to an applied magnetic field. The magnetic susceptibility, χ , indicates the effectiveness of an applied field to induce a magnetic dipole. It is defined as a ratio of the induced magnetization, M , and the applied field, H : $\chi = M/H$. Accordingly, the behavior of materials in a magnetic field can be classified as follows:

(1) Diamagnetism: diamagnetism is a basic property of all substances. For a diamagnetic substance, the interactions with an external field are weakly repulsive. Diamagnetic substances exhibit very low, negative susceptibilities ($\chi \approx 10^{-5}$ to 10^{-6}).

(2) Paramagnetism: in a paramagnetic material there are unpaired electrons, whose magnetic moments will tend to align in the same direction as the applied field. For paramagnetic materials, $\chi \approx 10^{-3}$ to 10^{-5} .

(3) Ferromagnetism: in ferromagnetic materials, electron spins on metal atoms are coupled into a parallel alignment that persists overall thousands of atoms into magnetic domains. Particles below a critical size can consist of a single domain. Below the Curie temperature, T_C , the forces of magnetic attractions are larger than thermal fluctuations (kT). The net magnetic moment can be very high. For ferromagnetic materials (nickel, iron, cobalt, gadolinium and their alloys), $\chi \approx 10^{-2}$ to 10^6 . The bulk materials of ferromagnetic substances are composed of many magnetic domains in each of which all the spins point to the same direction and act in a cooperative fashion. When the materials' size is decreased below a critical diameter, they become single-domain particles.¹ The critical diameter for the common ferromagnetic material iron is estimated to be 14 nm. Above the critical size, the materials show remanence, *i.e.* a persistent magnetization, and coercivity: a magnetic field in opposite direction is needed to demagnetize the material.

(4) Antiferromagnetism: in an antiferromagnetic substance, the electron spins of atoms in the crystalline lattice are fixed into an antiparallel alignment. Such substances have zero net magnetic moment, a small positive susceptibility ($\chi \approx 0-0.1$). Cobalt oxide (CoO) is an example of a well-known antiferromagnetic material.

(5) Ferrimagnetism: similar to ferromagnetic materials, a strong net dipole moment is present in the ferrimagnetic

substances despite an antiparallel alignment of nonequivalent spin moments. Magnetite (Fe_3O_4) is an example of a ferrimagnetic material. The critical diameter of a single domain of magnetite is estimated as 128 nm.

(6) Superparamagnetism: when the size of ferro- or ferrimagnetic particles is even smaller than a single domain, thermal fluctuations can cause the direction of magnetization to undergo Brownian rotation, *i.e.* thermal fluctuations prevent the existence of a stable magnetization. This state is called superparamagnetic because the particle behaves similarly to a paramagnetic spin but with a much higher moment. At a critical temperature, referred to as the blocking temperature, T_b , the dipole moments in the nanoparticle are able to align and couple to generate a large net induced magnetization. Above T_b , thermal fluctuations dominate and the material rapidly loses coupling of unpaired spins. Thus, they typically do not show any coercivity or remanence at room temperature. For magnetite a size of *ca.* 25 nm is necessary to obtain ferromagnetic behavior at room temperature.

Most magnetic materials possess anisotropic properties, which have great impact on their magnetization behavior. The coercivity is highly related to their anisotropic properties. Crystal anisotropy and shape anisotropy are the most important ones for nanostructured particles. The direction which can minimize the energy of a single nanocrystal's magnetization vector is called the easy axis. The anisotropy is thus determined by the chemical nature and crystal structure of a specific material. For polycrystalline materials, their magnetization behavior is strongly dependent on the shape, which is termed shape anisotropy. Spherical polycrystalline materials are composed of many single crystals which carry easy axes in every direction. So these materials do not show net crystal anisotropy at all since they are averaged in all orientations. However, non-spherical polycrystalline materials, such as cylinders or wormlike materials, are easier to be magnetized along the long direction than along the short one. Shape anisotropy is generally considered to impose the strongest influence on the magnetization property.¹ The 1D magnetic nanomaterials we will discuss in this review are either intrinsically cylindrical/wormlike materials (single- or polycrystalline nanowires, nanorods and nanotubes) or encapsulated spherical nanoparticles in 1D templates. In the latter case, if the particles are far from each other in a 1D template, the magnetization of the whole 1D nanoobjects is the collective contribution of individual particles.

The inorganic magnetic materials we discuss in this review cover ferro-, ferri-, and superparamagnetic nanomaterials, which strongly respond to external magnetic fields. Some 1D hybrid antiferromagnetic nanomaterials are also mentioned in spite of their small and positive susceptibility. Most organic materials, in particular polymers, are diamagnetic. However, in hybrid materials they can provide the magnetic particles chemical and physical stabilities, functionalities, responsiveness to environments, or biocompatibility. The combination at the nanoscale of a magnetic component with active organic species in a 1D manner gives rise to a new area of materials science and is supposed to be beneficial for the design and synthesis of multi-functional materials. Generally, the interest and demand for 1D organic-inorganic magnetic hybrid



Axel H. E. Müller

Axel H. E. Müller obtained his PhD in 1977 at the Johannes Gutenberg University in Mainz, Germany, working with G. V. Schulz. Since 1999 he has been professor and chair of Macromolecular Chemistry at the University of Bayreuth. In 2004 he received the IUPAC MACRO Distinguished Polymer Scientist Award. He is a Senior Editor of Polymer. His research interest focuses on the design of well-defined polymer structures by controlled/living polymerization techniques and on self-organized organic and hybrid nanostructures obtained from them.

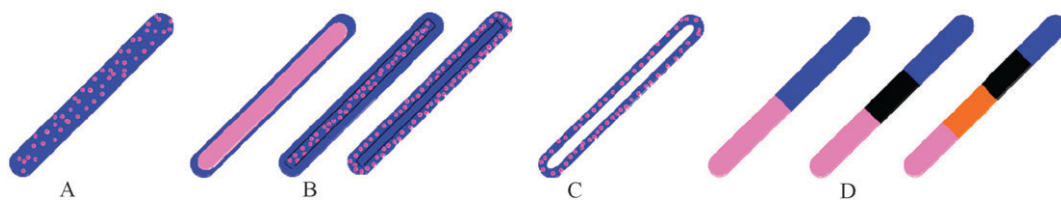


Fig. 1 Common structures of 1D inorganic–organic magnetic hybrid nanomaterials. (A) Magnetic nanoparticles (magenta) scattered in the organic phase (blue); (B) core–shell structure; (C) hybrid nanotubes; (D) block-type hybrids with 2, 3 or 4 blocks.

nanomaterials stems from the following factors: (i) compared with their inorganic counterparts, which easily agglomerate due to magnetic dipole interaction as well as high surface tension, 1D hybrid magnetic nanomaterials coated with organic layers, usually polymers, on the surface prevent a direct contact of the magnetic objects and improve their stability either in bulk or in solution. Effective coating with polymers enables easy processing and addressing of individual nanostructures. This is especially obvious in solution, because the shell polymers (usually charged polyelectrolytes) tethered to individual 1D object repel each other through steric or electrostatic repulsion. This is crucial for the fabrication of nanodevices from a single 1D object. (ii) By combining organic and magnetic components in a controlled manner, the complexity and functionality can be considerably enhanced. The synergetic relationship between the organic and magnetic parts can broaden the application spectrum of 1D nanomaterials. For instance, a magnetic 1D inorganic structure turns optically active when some chromophore is bound to the surface through the ligands. Besides, the stimuli-responsive behavior of some polymers might be incorporated into the 1D structure to make them “smart” and suitable for the task where feedback to external environment variations is needed. (iii) New properties and hierarchical architectures of 1D nanomaterials, which do not exist in any building block, can be attained through the interfacial interaction among the organic and/or inorganic phases in a 1D hybrid. It is not a fact of accumulating functions or properties into a single structure but of creating new ones. For instance, when 1D hybrid magnetic nanomaterials are synthesized *via* the assembly of individual magnetic nanoparticles crosslinked or immobilized by polymers, the orientation of the overall 1D object will be limited to its long axis. (iv) Due to the existence of the magnetic particles, the hybrid materials can be manipulated and easily separated/recovered by an external magnetic field. They can also be used as the contrast materials for magnetic resonance imaging (MRI), or the heating agents by high-frequency magnetic fields. (v) Finally, 1D inorganic–organic nanostructures are often necessary intermediates for the preparation of pure inorganic magnetic nanomaterials. Fig. 1 describes the common structures of 1D magnetic hybrid materials.

2. Synthetic strategies

Unlike the intensive research on spherical magnetic nanoparticles, the studies of 1D (rod-, wire- or tube-like) inorganic or hybrid magnetic nanomaterials came with an appreciable delay as a result of the difficult shape control and precise phase

distribution at an extremely small size. To favor the anisotropic formation of the materials at the nanoscale, physically or chemically forced oriented growth conditions are required. Benefiting from the latest advance in the field of low-dimensional nanostructures, 1D magnetic hybrids have attracted considerable attention. Initial efforts have aimed to handle their preparation and make use of their unusual properties and functions. Numerous methods and techniques have so far been developed to fabricate these nanomaterials. The major ones include template-directed synthesis, electrospinning, and 1D conjugation of building blocks, which will be discussed in details in the following sections.

2.1 Template-directed synthesis

In the context of materials chemistry, a template is a structure-directing agent. The template-directed method, allowing the transfer of a desired topology provided by the surface of a template, is a conceptually simple, intuitive, straightforward, and versatile route. It is therefore the most frequently used one for the formation of 1D magnetic hybrid nanomaterials. The shape and dimension of the resulting nanostructures can be readily tuned by choosing appropriate templates. Templates, according to their physical state, are generally classified into two types: “hard” and “soft” ones. Hard templates are made up of rigid materials with interior channels. An apparent advantage of a hard template is its superior control over the size and uniformity of the aimed 1D nanostructures. Ordered porous systems, such as anodic aluminium oxide (AAO) membranes, can generate uniform 1D magnetic nanostructures in a well-aligned regular array. This stirs great interest to study the ordering effect of 1D nanomaterials. However, the preparation of such templates is a tedious and time-consuming task, which is often expensive and difficult to scale up. Soft templates are commonly composed of (bio)-polymers and surfactants, and exist in a good many forms, such as superstructured polymeric nanostructures, unimolecular cylindrical brushes, and biological macromolecules. They can be incorporated with the magnetic phase in the final hybrid to afford a specific function, for example, solubilizing the nanostructures, introducing optical response or tuning surface properties (hydrophobicity or biocompatibility). It can be eliminated as well at an elevated temperature to afford pure inorganic magnetic materials, *i.e.*, the hybrid acts as an intermediate. In the following sections, we introduce several common templating methods, including channels in solids, mesostructures self-assembled from block copolymers, unimolecular cylindrical polymer brushes, biological superstructures, and other existing 1D objects.

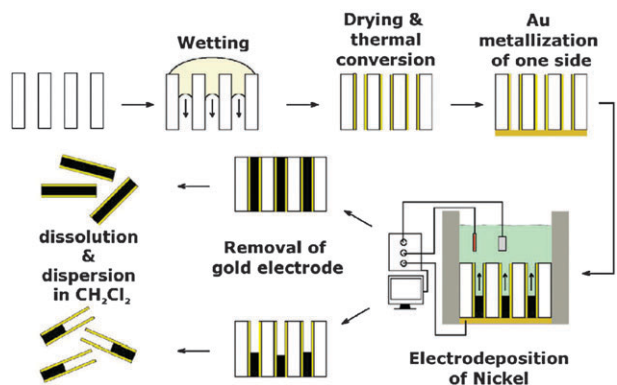


Fig. 2 Synthetic procedure of coaxial polymer–nickel hybrid nanowires with inner long or short metallic segments in polycarbonate membranes.² Reprinted with the permission of IOP Publishing Ltd.

2.1.1 Channels in solids. AAO and polycarbonate membranes are common hard templates for 1D nanomaterials. To generate a magnetic 1D hybrid, a magnetic precursor and the organic materials are sequentially or simultaneously filled into the pore before further processing. An example of the preparation of coaxial nickel/poly(*p*-phenylene vinylene) (PPV) hybrid nanowires in polycarbonate membranes is illustrated in Fig. 2.² The synthetic procedure involved two steps. The first step consisted in wetting a porous polycarbonate membrane ($L \approx 50 \mu\text{m}$, $D \approx 130\text{--}150 \text{ nm}$) with a sulfonium polyelectrolyte, a precursor polymer of PPV. After thermal conversion of the precursor impregnated in the template at $110 \text{ }^\circ\text{C}$, PPV nanotubes formed. In the second step, considering the PPV-coated membrane as a secondary template, an electrochemical method was used to fill the inner channel of the PPV nanotubes with nickel. This required the coating of a gold layer on one side of the membrane that acted as a working electrode. Nickel was deposited from an aqueous solution containing a nickel salt at $\text{pH} \approx 4$. The electrodeposited nickel then grew from bottom to top in the hollow interior of PPV nanotubes. The length of the nickel segment (short and long) was controllable by the electrodeposition process. After removal of the gold electrode and selective dissolution of the membrane in dichloromethane, free-standing polymer–nickel nanowires were obtained with luminescent properties arising from the optically active PPV shell. The morphology of coaxial PPV–Ni nanowires was confirmed by high magnification scanning electron microscopy (SEM) image. The diameter of the coaxial nanowire was typically $130\text{--}150 \text{ nm}$, the same as that of the membrane pores. The shell was a rough sheath of $20\text{--}40 \text{ nm}$ covering a metallic core with a diameter of $90\text{--}110 \text{ nm}$. In spite of the external roughness of the PPV shell, the metallic nickel core was very smooth. Additionally the polymer shell seemed to prevent nickel from oxidation.

Using the same template, polymer–magnetic nanotubes have been prepared by Layer-by-Layer (LbL) assembly of polyelectrolytes and magnetic nanoparticles.³ The polymeric nanotubes were fabricated through the alternating LbL assembly of poly-L-lysine hydrochloride (PLL) and poly-L-glutamic acid (PGA). The wall thickness and inner diameter of as-prepared nanotubes were tunable by changing the

assembled layers. After the formation of polymeric nanotubes in the porous membrane, citrate-stabilized magnetic nanoparticles (negatively charged) were deposited into the inner layer of PLL/PGA multilayers on the template. The inner layer of the nanotubes contained magnetite nanoparticles, which allowed the magnetic manipulation of these tubes in solution, while the outer layer could be designed to load and release gene molecules.

Compared with the polycarbonate membrane, the pores in the AAO template are more uniform, regular and with a small tilting angle. Mirkin *et al.* first reported a synthetic strategy in which Au–polypyrrole (PPy) or Au–PPy–Au segmented metal–polymer nanorods were prepared by electrodeposition of gold into porous alumina membranes, followed by electrochemical polymerization of pyrrole.⁴ Taking advantage of this strategy, a hybrid multisegmented magnetic nanowire can be achieved by inserting in between a magnetic segment. Fig. 3 shows a gold–PPy–nickel–gold multisegmented nanowire that was synthesized in an AAO template by Myung *et al.*⁵ The segment sequence of Au–PPy–Ni–Au nanowires was adopted so that gold segments worked as the electrical contact and a PPy–Ni midsection for sensing and magnetic alignment, respectively. Initially, one side of the AAO template was sputter-coated with gold that served as the seed layer for electrodeposition. A three-electrode configuration was used to deposit segments of gold, PPy and nickel, respectively. After electrodeposition, the Au seed layer was mechanically removed, followed by dissolution of the AAO template in a concentrated aqueous solution of NaOH, which provided multisegmented hybrid magnetic nanowires.

Different from the stepwise loading mentioned above, polymeric and magnetic components can be introduced into the porous template in a single step. According to different infiltration methods, either polymer–magnetic nanotubes or nanofibers are accessible.⁶ Precursor–film–wetting infiltration

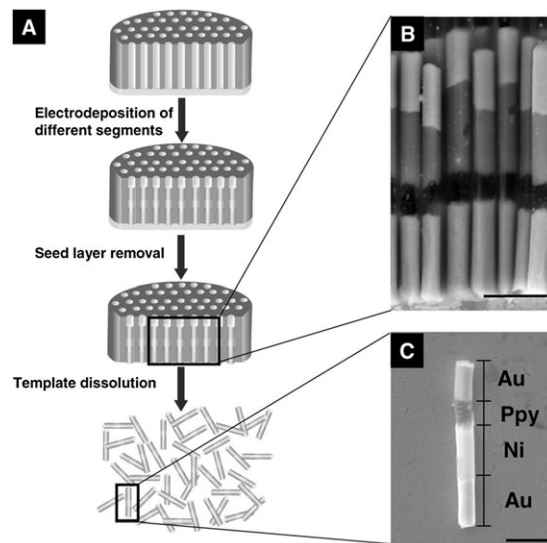


Fig. 3 (A) Procedure of the synthesis of Au–PPy–Ni–Au multisegmented nanowires. (B) Cross-sectional SEM image of four-segmented nanowires inside the alumina template. (C) SEM image of a single nanowire showing different segments of the nanowire (scale bar $\approx 1 \mu\text{m}$).⁵ Reprinted with the permission of Wiley-VCH.

is an efficient method for preparing polymer-based magnetic hybrid nanotubes. Nanotubes composed of polystyrene (PS) and $\text{Fe}_{50}\text{Pt}_{50}$ nanoparticles (3–4 nm) were prepared by melting a bulk PS/ $\text{Fe}_{50}\text{Pt}_{50}$ mixture on an AAO template (pore diameter ≈ 360 nm) at 200 °C. The nanotubes formed were 50 μm in length and 360 nm in diameter. The small size of the nanoparticles compared to the diameter of nanotubes (~ 70 nm) allowed for the convenient infiltration of nanoparticles dispersion in PS in a molten state. Besides the hybrid nanotubes, polymer-based magnetic nanofibers can be obtained *via* a solution-wetting-infiltration method. For instance, nanofibers composed of PS and $\text{Fe}_{50}\text{Pt}_{50}$ nanoparticles were prepared after submerging the porous template into a 10 wt% solution of PS/nanoparticle in toluene for 2 days. In addition, poly(vinyl alcohol)/ CoFe_2O_4 nanofibers with an aspect ratio above 2000 were prepared *via* a vacuum infiltration method.

2.1.2 Mesostructures self-assembled from block copolymers.

Block copolymers have been widely used as versatile and powerful soft templates for the fabrication of various nanomaterials with hierarchical architectures and complex functionalities. By means of self-assembly, either in solution or in the bulk, block copolymers undergo microphase segregation and generate different morphologies, among which polymer cylinders or tubes are of special interest for the fabrication of 1D nanostructures. To improve the stability of the polymer template in solution, crosslinking is often performed to chemically lock the cylindrical domains. Liu *et al.* synthesized crosslinked cylindrical polymer assemblies starting from a linear triblock terpolymer of polystyrene-*b*-poly(2-cinnamoyl ethyl methacrylate)-*b*-poly(*tert*-butyl acrylate) (PS-*b*-PCEMA-*b*-PtBA) in a solid state (Fig. 4).⁷ By casting and annealing of a thin film, the triblock terpolymer initially self-assembled into an array of core-shell cylinders with a

PtBA core and a PCEMA shell in a PS matrix (A \rightarrow B). The PCEMA, rich in vinyl groups, was photo-crosslinked in the bulk by UV light to fix the cylindrical shape (B \rightarrow C). Upon interaction with THF, a good solvent for the polymer, the crosslinked fibers were dispersed into solution (C \rightarrow D). In the following step the fibers were converted into nanotubes with interior carboxylic acid groups by the selective hydrolysis of the PtBA core into poly(acrylic acid) (PAA) (D \rightarrow E), which was a weak polyelectrolyte capable of coordinating metal ions. Through encapsulation of iron ions into the PAA interior, followed by alkalization, $\gamma\text{-Fe}_2\text{O}_3$ nanoparticles were *in situ* generated within the polymeric nanotubes. Since the nanoparticles were exclusively in the interior of the nanotubes, the well-defined 1D magnetic hybrids have desired stability in solution. In an improved procedure by the same group, water-soluble polymer nanotubes were prepared *via* self-assembly of a hydrophilic triblock copolymer in water, which in turn were used as templates to fabricate Pd/Ni nanoparticles in the tubular core.⁸

Winnik and Manners *et al.* reported that block copolymers with a semicrystalline, iron-containing core-forming poly(ferrocenyldimethylsilane) (PFS) block readily formed cylindrical micelles in selective solvents over a wide range of compositions.⁹ Without any crosslinking procedure, the cylinders could be readily employed as templates for the formation of 1D magnetic hybrid nanostructures because the crystalline core at room temperature was in a solid state that firmly held the cylindrical shape of block copolymer assemblies. As illustrated in Fig. 5, a diblock copolymer $\text{PFS}_{17}\text{-}b\text{-P2VP}_{170}$ (polydispersity index, 1.07. P2VP: poly(2-vinylpyridine)) was prepared using a sequential living anionic polymerization approach. Cylindrical micelles up to 10 μm in length and 30 nm in width (PFS core ≈ 10 nm), which contained a core of PFS and a corona of P2VP, were prepared by self-assembly of the block copolymer $\text{PFS}_{17}\text{-}b\text{-P2VP}_{170}$ in 2-propanol, a

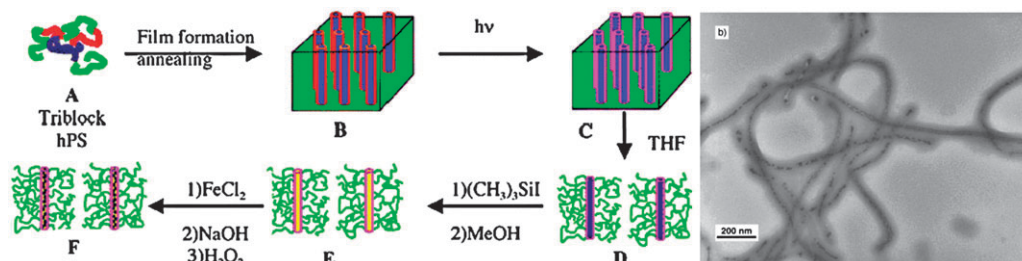


Fig. 4 Synthetic strategy (left) and TEM image (right) of the PS-*b*-PCEMA-*b*-PAA triblock terpolymer/ $\gamma\text{-Fe}_2\text{O}_3$ hybrid magnetic nanofibers.⁷ Reprinted with the permission of Wiley-VCH.

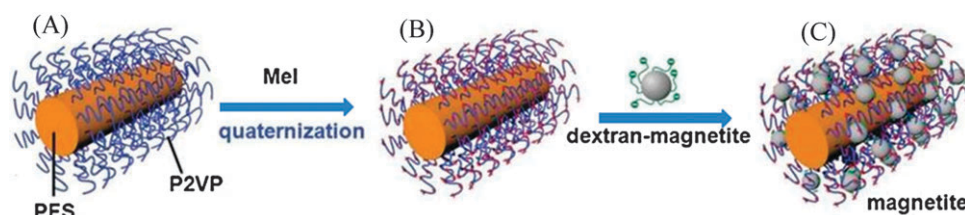


Fig. 5 Template-directed synthesis of hybrid magnetic nanowires using $\text{PFS}_{17}\text{-}b\text{-P2VP}_{170}$ diblock copolymer cylindrical micelles. (A) Self-assembled micelles, (B) micelles with a cationic corona derived from quaternization of P2VP with methyl iodide (MeI), and (C) polymer-magnetite nanowires.⁹ Reprinted with the permission of Wiley-VCH.

selective solvent for the P2VP block. The cylinders became positively charged *via* a quaternization reaction of the P2VP corona with methyl iodide in 2-propanol. The charged surface on the polymer cylinders favored an electrostatic interaction with dextran-functionalized magnetite nanoparticles, giving rise to hybrid magnetic nanowires with a dense outer shell of magnetic nanoparticles.

2.1.3 Cylindrical polymer brushes. A cylindrical polymer brush (CPB) refers to a polymer possessing densely grafted side chains on a linear long polymer main chain. Compared with polymer cylinders generated from block copolymer self-assembly mentioned above, cylindrical polymer brushes are single macromolecules with extended chain conformation in dimensions of up to several hundreds of nanometres. Among various morphologies, core-shell cylindrical brushes which contain amphiphilic diblock copolymer side chains are of special interest, because an intramolecular phase separation in solution creates a 1D nanochannel in the core surrounded by a protective shell. The anisotropically shaped core can be practically used as a nanoreactor to synthesize and accommodate 1D magnetic nanostructures. The fabrication of superparamagnetic maghemite ($\gamma\text{-Fe}_2\text{O}_3$) nanocylinders from amphiphilic polymer brushes is illustrated in Fig. 6. The PAA block, which possessed carboxylate groups, was capable of coordinating with iron ions (*e.g.*, Fe^{2+} , Fe^{3+}). It worked as a nanoreactor to generate nanoparticles and linearly aligned them along the brush core; the hydrophobic shell, poly(*n*-butyl acrylate) (P*n*BA), free of interaction of the

metal precursors provided the solubility of the whole hybrid cylinders. In the first step (a to b), the carboxylic acid functions in the PAA core were neutralized by NaOH to afford a strong cationic polyelectrolyte core. The sodium ions were substituted by Fe^{2+} or Fe^{3+} in an ion exchange process (step 2: b to c), forming polychelates (composites of polymer brush and iron ions) in which the metal precursors were immobilized. Through alkalization, the iron ions within each polychelate were converted to $\gamma\text{-Fe}_2\text{O}_3$ nanoparticles that were simultaneously aligned and fused into a 1D manner within the cylindrical core (step 3: c to d). Transmission electron microscopy (TEM) is a suitable characterization method to monitor the fabrication process. Pure polymer brushes appeared transparent due to insufficient contrast. When polychelates were formed, the iron ions with high electron density stained the brush core, making it visible. As shown in Fig. 6g and h, wire-like dark objects were clearly observed after the uptake of Fe^{3+} ions. A TEM image with higher magnification showed the presence of a “pearl-necklace” structure, which was due to the crosslinking of the PAA side chains by iron ions. After converting the iron ions to iron oxide nanoparticles, crosslinking of the PAA side chains *via* ions vanished, consequently the “pearl-necklace” structure disappeared. Fig. 6e and f showed the TEM images of as-prepared superparamagnetic hybrid nanocylinders with smooth contour.

As mentioned above, superparamagnetic hybrid nanocylinders were prepared by the *in situ* generation of maghemite nanoparticles within CPBs possessing a PAA core and a P*n*BA shell. Because of the amphiphilic nature of CPBs, a mixture of

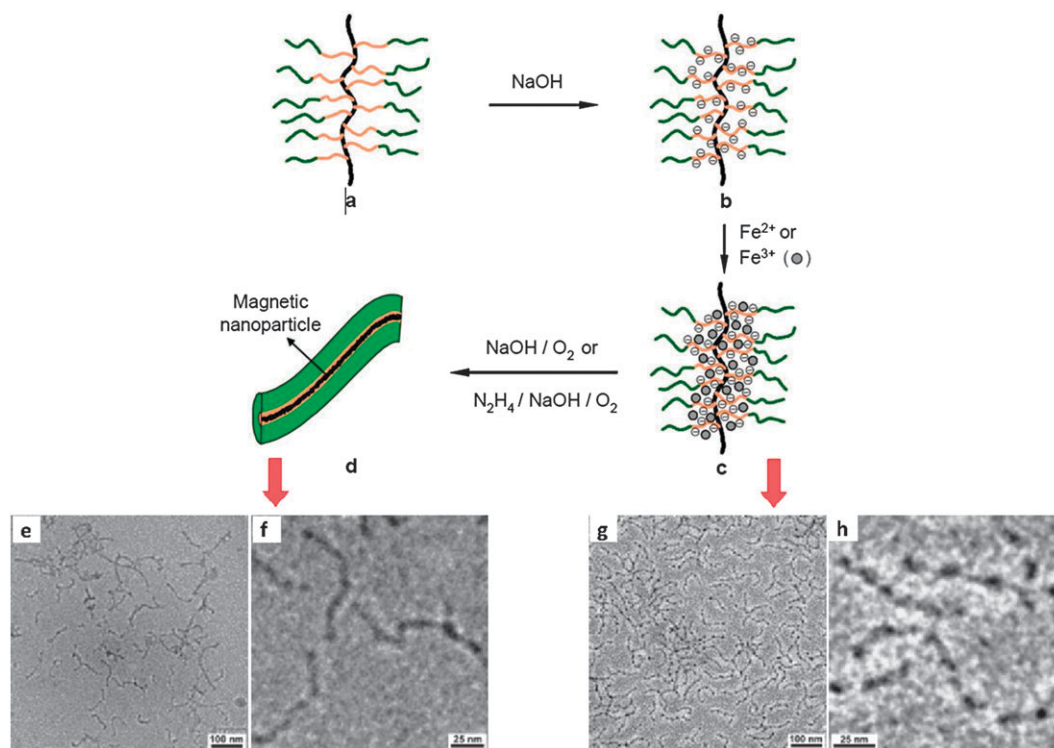


Fig. 6 Synthesis of an iron oxide ($\gamma\text{-Fe}_2\text{O}_3$) hybrid nanowire templated by an amphiphilic cylindrical polymer brush: (a) brush with a PAA core and a P*n*BA shell; (b) neutralized polymer brush with a poly(sodium acrylate) core; (c) polychelate of the brush with Fe^{2+} or Fe^{3+} ions; (d) hybrid nanocylinder; (e, f) TEM images of the as-synthesized hybrid magnetic nanocylinders ($[\text{AA}_{37}\text{-}b\text{-}n\text{BA}_{48}]_{1500} + \gamma\text{-Fe}_2\text{O}_3$); (g, h) TEM images of the polychelate of brush $[\text{AA}_{25}\text{-}b\text{-}n\text{BA}_{61}]_{1500}$ and Fe^{3+} ions.¹⁰ Reprinted with the permission of Wiley-VCH.

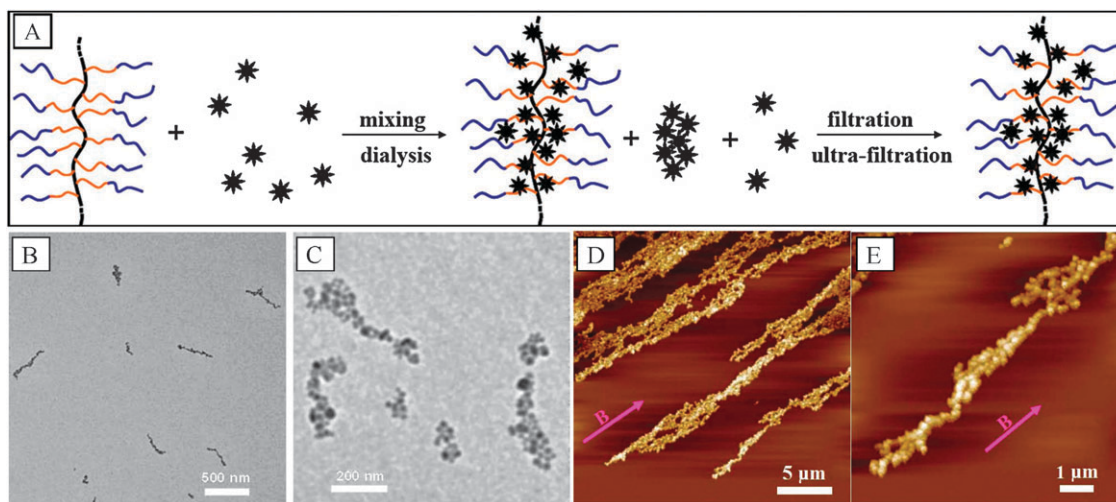


Fig. 7 (A) Synthetic route to water-soluble superparamagnetic hybrid nanocylinders templated by core-shell cylindrical brushes via an “introducing into” strategy. (B, C) TEM images of the nanocylinders. (D, E) AFM height images of the hybrids aligned on a mica surface in a magnetic field of 40 mT, Z range: 50 nm.¹¹ Reprinted with the permission of Wiley-VCH.

organic solvents (chloroform + methanol) was used to disperse the hybrids, which were inconvenient for practical handling. Besides, the magnetic nanoparticles generated *in situ* in the core of the CPBs were only 2 to 3 nm in diameter, therefore the magnetic response was relatively weak. In an improved approach, a new “introducing into” strategy, as shown in Fig. 7A, was developed by the same group to overcome these drawbacks.¹¹ A water-soluble bis-hydrophilic CPB with a poly(methacrylic acid) (PMAA) core and a poly(oligo(ethylene glycol) methacrylate) (POEGMA) shell was first prepared. Presynthesized magnetite (Fe_3O_4) nanoparticles with an average diameter of 10 nm were mixed with an aqueous solution of brushes. It was found that the nanoparticles were able to penetrate the POEGMA shell and insert into the brush core. Excessive nanoparticles that remained free in solution were removed by ultrafiltration. The purified hybrid nanocylinders (Fig. 7B) showed a linear arrangement of the magnetite nanoparticles, which agreed with the cylindrical morphology of CPBs. They were readily aligned (Fig. 7D and E) when dried from solution onto a solid substrate in the presence of a weak external magnetic field (40–300 mT).

Morphologically, the CPBs are similar to cylindrical micelles self-assembled from surfactants or block copolymers in solution. Since the side chains are covalently bound to the main chain in CPBs, they exhibit a superior stability with regard to self-assembled cylinders against external stimuli such as solvent and pH. In addition, their size distribution can be efficiently controlled in a polymerization process. However, the length of all present CPBs is limited below 1 μm .

2.1.4 Biological 1D templates. Nature offers a multitude of biological nanostructures with unmatched complexity and functionality. They control the daily mineralization and nanocrystal synthesis in exact shapes and sizes with high reproducibility and accuracy under mild reaction conditions. In certain examples, the building blocks are organized preferentially into a 1D manner. These originally elongated biologic supramolecules can be harvested from environment

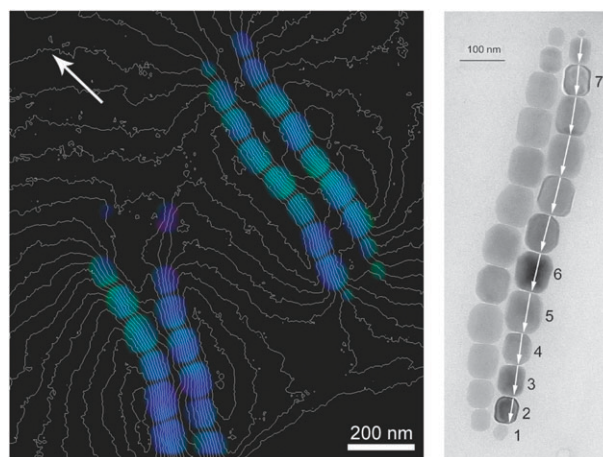


Fig. 8 Left: magnetic induction map from two pairs of bacterial magnetite chains at 293 K. The magnetic field lines are oriented so that the vector points toward the northwest in the image. Right: a typical bright-field TEM image of a double chain of magnetite magnetosomes from a single bacterial cell.¹³ Reprinted with the permission of IOP Publishing Ltd.

and used as templates for the fabrication of nanostructures. Within a largely diamagnetic background of these biological systems, magnetotactic bacteria stand for an exception. They contain magnetosomes (the magnetic nanoparticles and the associated phospholipid vesicle), which are intracellular, ferromagnetic crystals of magnetite or greigite (Fig. 8).^{12–14} The mineralization processes are highly regulated, resulting in the formation of uniform magnetic nanoparticles that are usually arranged in one or more linear chains along the chain axis within each bacterium. Thus, the bacterium itself is a natural living 1D magnetic hybrid. The crystals in magnetotactic bacteria have specific morphologies within each cell type, and their magnetic axes are usually aligned. The small sizes of the crystals (40–100 nm) suggest that they should each contain a single magnetic domain and magnetic interactions between particles are oriented along the chain. It imparts a

permanent large magnetic moment to the cell that enables the bacterium to sense and migrate along geomagnetic field lines, maintaining its position within the interface of the oxy–anoxic zone. This behavior is thought to increase the efficiency with which such bacteria find their optimal oxygen concentrations or redox potentials at sediment water interfaces or in water columns.

DNA is among the most famous natural 1D templates. Many efforts have been devoted for generation of magnetic hybrid nanowires from DNA strings. These efforts can be roughly classified as two strategies: external introduction of a magnetic nanoparticle or *in situ* metallization. In the first strategy, magnetic nanoparticles and DNA are mixed to afford the insertion of nanoparticles into the DNA strands.^{15,16} For instance, DNA–Fe₂O₃ hybrid nanowires were prepared by incubation of a solution of double-stranded nonmethylated λ -phage DNA in buffer in the presence of Fe₂O₃ nanoparticles. In the second strategy, DNA is metallized with magnetic metals in three sequential steps: (1) the binding of metal ions or metal complexes to DNA strands. This activation step is based on either exchanging ions with the DNA backbone or the insertion of metal complexes between the DNA bases. (2) Reduction of reactive metal sites. This forms metal nanoclusters attached to the DNA strand. (3) The autocatalytic growth of these affixed metal nanoclusters, which are able to act as seeds because of the simultaneous presence of both metal ions and reducing agents in the growth solution. In this step, a second metal ion could be deposited on the DNA scaffold. For example, Co nanoparticles could grow on the Pt nanoseeds in the third step to form magnetic Co nanowires on the DNA.^{17,18}

Besides DNA, several viruses have been used as biological templates for the fabrication of 1D magnetic hybrid or other nanostructures. A famous example is tobamovirus, a plant virus. Tobamovirus particles are 300 nm in length with outer and inner diameters of 18 and 4 nm, respectively (Fig. 9A and B). The internal and external surfaces consist of repeated patterns of charged amino acid residues, such as glutamate, aspartate, arginine, and lysine. Tobacco mosaic virus (TMV) and tomato mosaic virus (ToMV) are two common species of the tobamovirus. Mann *et al.* demonstrated TMV as a template for the fabrication of iron oxide nanoparticles on the TMV external surface at mild pH conditions by specific metal ion binding onto the numerous glutamate and aspartate

surface groups.¹⁹ The biomineralization on the surface of a protein resulted from the electrostatic interactions between source ions and the protein surface. In the case of cage-shaped proteins, it has been proposed that highly condensed source ions created nuclei and the inner surface of the protein acted as a self-catalyst. The importance of a nucleation site has also been demonstrated by exposing clusters of four negatively charged glutamic acid residues as nucleation sites on the outer surface of bacteriophage M13, which resulted in the formation of antiferromagnetic Co₃O₄ nanoparticles.²⁰ Utilizing the central channel of TMV, the formation of Ni, Co, Co/Pt, and Fe/Pt nanoparticles has been reported. The inner surface of ToMV consists of helically stacked coat proteins, and only a limited number of amino acid residues face the central channel. To overcome this limitation, Yamashita *et al.* modified ToMV genetically to introduce point mutations in the region facing the inner surface of ToMV so that the number of positive (lysine: K) or negative (aspartic acid: D) charges were increased in order to generate additional nucleation sites.²¹ It turned out that increasing the positive charge at a specific site offered more sites for nucleation, resulting in the growth of aligned nanoparticles inside the virus (Fig. 9D).

2.1.5 Templating against other existing 1D objects. Existing inorganic or hybrid 1D objects are ready-made templates. From an inorganic magnetic 1D nanostructure, a hybrid is generated easily by surface-functionalization with polymer layers, which forms a coaxial nanocable structure. As a highly versatile approach, LbL assembly can be adopted to graft polymers onto an inorganic surface. The major advantage of this technique is that the thickness, morphology, and composition of the targeted materials can be controlled by varying the number of the polymer deposition cycles and the composition of the layer component (*e.g.*, polyelectrolytes, nanoparticles, precursor molecules, *etc.*). Taking advantage of the LbL colloid-templating approach, Caruso and co-workers succeeded in the preparation of polymer–nickel core–shell magnetic nanocables.²² The assembly process was based on the electrostatic interaction of two oppositely charged polyelectrolytes poly(diallyldimethylammonium chloride) (poly-DADMAC) and poly(sodium 4-styrenesulfonate) onto a nickel nanorod surface. Besides polyelectrolytes, a combination of a polyelectrolyte and a titania precursor as the

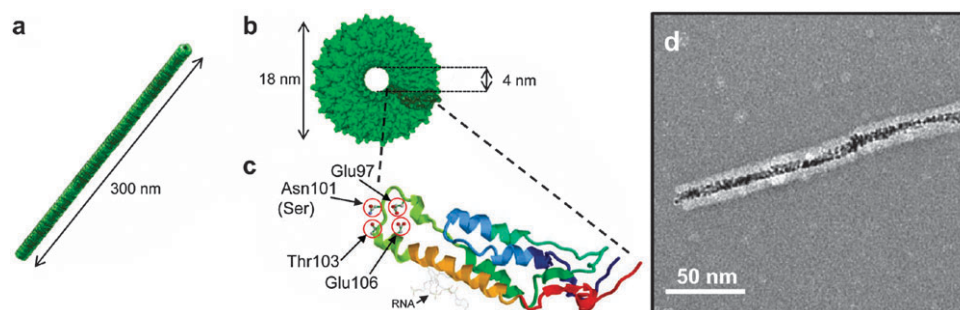


Fig. 9 (a) Schematic illustration of tobamovirus. (b) Top view of the virus. (c) Atomic coordination of a coat protein subunit of the virus (PDB:2OM3) prepared with PyMol. (d) TEM image of aligned nanoparticles (Pt/Co) formed inside mutants.²¹ Reprinted with the permission of ACS.

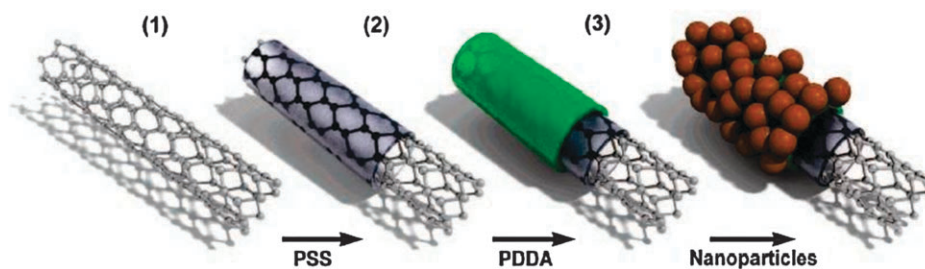


Fig. 10 Schematic illustration of the deposition of magnetite nanoparticles on CNTs based on polymer wrapping (1) and LbL assembly (2, 3).²³ Reprinted with the permission of ACS.

depositing partners allowed to coat a titania–polyelectrolyte hybrid shell around the nickel nanorod.

In a slightly modified deposition protocol, this approach can be virtually extended to prepare 1D hybrid magnetic nanomaterials from all 1D inorganic templates. As a classic example, carbon nanotubes (CNTs) are one of the most fascinating nanomaterials with a wide range of applications. A simple procedure for the preparation of hybrid magnetic CNTs was reported based on the LbL assembly of polyelectrolytes and magnetic nanoparticles onto the surface of CNTs.²³ The method combines the polymer wrapping and LbL assembly techniques allowing the noncovalent attachment of nanoparticles onto the carbon nanotubes and thus leaving intact their structure and electronic properties. A typical procedure of the assembly process is illustrated in Fig. 10. Poly(sodium 4-styrene sulfonate) was used as a wrapping polymer providing remarkably stable aqueous dispersions of multiwalled CNTs. Because of the high density of sulfonate groups on the anionic polyelectrolyte, it acted as a primer onto the CNTs surface for the subsequent, homogeneous adsorption of the cationic polyelectrolyte poly(DADMAC) through electrostatic interactions, which in turn provided a homogeneous distribution of positive charges onto the CNTs surface. These positive charges ensured the efficient adsorption of negatively charged magnetic nanoparticles onto the surface of CNTs by means of electrostatic interactions.

1D hybrids can serve as templates as well. It has been reported that polymer-coated tellurium (Te) nanorods were used to assemble oleic acid-capped magnetite nanoparticles ($d \approx 9.8$ nm) onto their surface in an organic solvent, THF, which formed a colloiddally stable magnetic nanocylinder (Fig. 11).^{24,25} The assembly procedure was very straightforward by mixing two component solutions of polymer–tellurium nanorods and magnetite nanoparticles in THF under

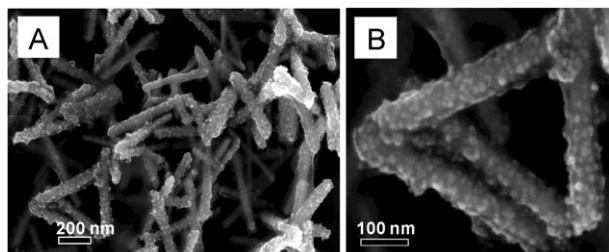


Fig. 11 SEM image of magnetic nanocylinders based on the assembly of oleic acid-stabilized magnetite nanoparticles on polymer coated Te nanorods.²⁵ Reprinted with the permission of ACS.

mechanical shaking. During this process, all nanoparticles below a critical concentration assembled themselves onto the nanorod surface *via* an interaction between the polymer layer on the nanorods and the alkyl chains on the nanoparticles. This approach of generating 1D magnetic hybrid nanostructures is very unique with the following advantages: (1) no purification or post-treatment was required in the case of a suitable concentration of nanoparticles. All nanoparticles are attached to the nanorods statistically, leaving magnetic nanocylinders as the only product in solution. (2) A desired magnetic moment of the nanocylinders was achievable *via* an appropriate stoichiometric ratio of nanoparticles to nanorods. (3) The size and aspect ratio of the magnetic nanocylinders stemmed from the Te nanorods, which were effectively controlled at different reaction conditions. (4) Due to the protective polymer and surfactant layer on their surface, these nanocylinders were well-dispersed in organic solvents.

In general, the template approach produces all possible structures of 1D magnetic hybrid nanomaterials presented in Fig. 1. Templates, ranging from inorganics, hybrids, synthetic polymers as well as natural biopolymers, play the effective role of structure directing agents to spatially control the deposition and organization of magnetic components. Within each type of templates, several physical or chemical processes are involved, such as electrodeposition, self-assembly, adsorption, complexation, chemical reactions, *etc.* Each of these templates as well as the process chosen governs different structural parameters (size, shape, crystallinity, mutual interaction, *etc.*), and demonstrates distinct advantages with respect to the materials design, as well as limitations from a synthetic perspective. For example, 1D magnetic hybrid nanomaterials prepared from AAO templates are usually more rigid, smooth and continuous than that from synthetic and biopolymers. Even using the same template of AAO membranes, the sequential filling of magnetic moieties with polymers into the channels gives multicompartmented nanostructures, while simultaneous filling uniformly disperses magnetic species into a polymer matrix. In addition, compared to “hard” templates, “soft” ones are easier and more cost-effective to scale up the production of 1D nanomaterials, especially in the case of some biopolymers that can be directly harvested from nature.

2.2 Electrospinning

Electrospinning has been actively explored as a versatile and simple method to process polymer-containing solutions or melts into continuous fibers. Compared with other methods,

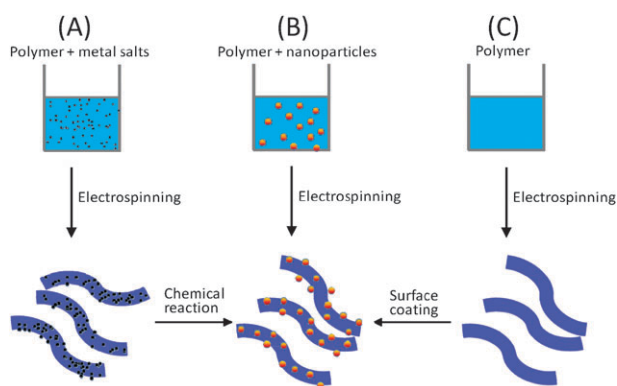


Fig. 12 Illustration of three basic methods to prepare hybrid magnetic nanofibers by electrospinning.

currently electrospinning is the only technique that allows the fabrication of continuous ultralong fibers with diameters down to a few nanometres. There are chiefly 3 types of electrospinning processes involved in the preparation of 1D magnetic hybrid nanomaterials (Fig. 12). In process A, a polymer solution with metal salts is electrospun to form hybrid nanofibers with metal salts uniformly distributed in the polymer matrix. *Via* gas phase chemical reactions the metal salts are *in situ* converted to magnetic nanoparticles within the polymer nanofibers. As an example, polymer/iron oxide nanofibers were prepared by *in situ* generation of iron oxide nanoparticles within the PEO nanofibers *via* the reaction of the traveling jet (PEO + iron salts) with an active atmosphere, ammonia gas.²⁶ The magnetic nanoparticles prepared in this method however are less crystalline due to the limited reaction conditions, such as low temperature. In fact, electrospinning of polymer solution with additives, such as metal salts, is more popular for the preparation of pure inorganic nanowires by calcination of the hybrid nanofibers at elevated temperature to develop desired properties of the inorganic components.²⁷ Process B represents the main stream of the current preparation methods of magnetic hybrid nanofibers *via* electrospinning. In this process, a polymer solution is blended with a given amount of magnetic nanoparticles. The magnetic nanoparticles can be added externally into the polymer solution or *in situ* generated. Given an appropriate ratio of polymer to nanoparticles, uniform magnetic nanofibers with homogeneous loading of magnetic nanoparticles can be obtained.²⁸ As an example, polyacrylonitrile–magnetite (PAN–Fe₃O₄) hybrid nanofibers with different loading concentrations of magnetite nanoparticle have been fabricated.²⁹ The challenges of particle dispersion and agglomeration were encountered during electrospinning at a high loading of nanoparticles. The net result was a high viscosity, which prevented a continuous jet and subsequent fiber formation. Compared with processes A and B, process C involves a polymeric nanofiber intermediate followed by surface functionalization with magnetic species. Thus, the electrospun polymer fibers serve as an existing 1D polymeric template to be converted to magnetic hybrids. The immobilization of iron nanoparticles onto a continuous nanofiber-based support through the combination of the LbL assembly approach with electrospinning technology has been reported.³⁰ For example,

electrospun cellulose acetate nanofibers were LbL-assembled with multilayers of poly(DADMAC) and PAA through electrostatic interaction. The formed polyelectrolyte multilayers coated onto the cellulose acetate nanofibers were used as a nanoreactor to complex iron ions through the binding with the free carboxyl groups of PAA. Subsequent reduction formed Fe nanoparticles immobilized in the polyelectrolyte multilayers around the fibers. Furthermore, in a LbL-free approach, electrospun PAA/poly(vinyl alcohol) nanofibrous mats were treated at an elevated temperature to render them water stable. They were subsequently used as nanoreactors to generate iron nanoparticles.³¹

Although electrospinning is a simple technique, it does provide hybrid nanofibers with various morphologies and functions. Many processing parameters as well as the instrument itself can be modified to obtain fibers with specific morphology. By electrospinning a block copolymer instead of a homopolymer, a phase separation took place in the as-synthesized nanofibers; magnetic nanoparticles could be selectively deposited onto desirable locations of the nanofibers.³² As a parallel approach, poly(styrene-*b*-isoprene) has been chosen as the polymer matrix for electrospinning with magnetic nanoparticles. Due to the inherent fast evaporation and strong deformation rates in the electrospinning process, the particles preferentially wetted the polyisoprene domain and at the same time remained monodisperse in spite of a high particle fraction (10%). In addition, very recently emerged coaxial electrospinning provides an alternative to design new functional hybrid nanofibers with core–shell structures. For instance, Zhang *et al.* reported the employment of coaxial electrospinning for encapsulation of an array of self-assembled iron–platinum nanoparticles along the axis of poly(ϵ -caprolactone) nanofibers.³³

2.3 1D conjugation of building blocks

Directional organization of magnetic nanoparticles in a linear manner in solution or on a solid substrate can create 1D magnetic hybrids as well. One-dimensional chains of nanoparticles exhibit unique magnetic properties due to geometric confinement, magnetostatic interactions, and nanoscale domain formation.^{34,35} Such systems also provide valuable insight into basic physical phenomena and the study of basic properties of nanoscale magnetism. In this synthetic approach, pre-synthesized inorganic or hybrid magnetic nanoparticles are controllably conjugated in a 1D fashion. The conjugation is driven by a magnetic dipole–dipole interaction between adjacent nanoparticles or a self-assembly process. The preparation and assembly of nanoparticles can proceed separately or simultaneously. In the second case, the nanoparticles are formed and assembled in a one-pot synthesis. The general advantage of such a linear attachment is that the diameter of the hybrid nanowire is chiefly governed by that of the nanoparticles. This facilitates the construction of magnetic hybrid nanowires with defined or ultrathin diameter down to a few nanometres.

It is well-known that surfactant mixtures of oleic acid, aliphatic amines, and trioctylphosphine oxide can be used to prepare well-defined magnetic nanoparticles. Pyun *et al.*

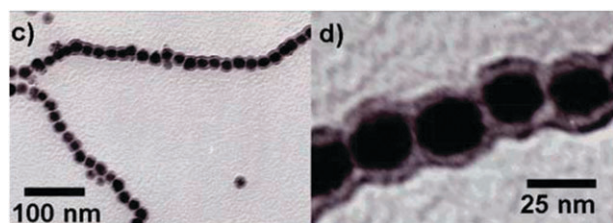


Fig. 13 TEM images of self-assembled single Co nanoparticle chains.³⁶ Reprinted with the permission of ACS.

expanded upon this concept by the preparation of end-functional polymeric surfactants bearing either an amine, or a phosphine oxide ligand terminus to mediate the growth of ferromagnetic cobalt nanoparticles.³⁶ The use of end-functional polymers combined the advantageous characteristics of polymers and small molecule surfactant systems, enabling the synthesis of highly uniform ferromagnetic colloids possessing a hairy corona of stabilizing polymer chains. Ferromagnetic cobalt nanoparticles of uniform diameter of 15 nm were prepared using this system. The self-assembly of these dipolar magnetic nanoparticles into chains (Fig. 13) was investigated in solutions cast onto supporting substrates. The local nematic-like ordering of polymer-coated nanoparticle chains was also observed along with a tendency of adjacent chains to form “zippering” configurations due to van der Waals interactions. In addition, by post-synthesis oxidation of cobalt, PS–cobalt oxide as well as PS–Au–cobalt oxide antiferromagnetic hybrid nanowires were generated by the same group.^{37,38}

Polymers other than polymeric surfactants have also been reported to form 1D magnetic chains from nanoparticles. Commonly the chains are first formed by aligning nanoparticles in solution assisted by an external magnetic field, and simultaneously the polymers behave as a strong linker to fix the chain morphology through the interpenetration and bridging of macromolecule layers. Once this process is completed, the polymer–nanoparticle magnetic chain remains in its anisotropic shape even when the magnetic field is cancelled. For example, unique legume-like structures of

superparamagnetic Co nanoparticles have been prepared through a simple polymer-assisted and magnetic-field-induced assembly method.³⁹ The magnetic field was employed to arrange cobalt nanoparticles along the lines of magnetic force in a head-to-tail configuration in solution; the polyvinylpyrrolidone polymer, besides its function as a coordinating and stabilizing agent in the formation of nanoparticles, acted as a “glue” to permanently hold the 1D nanostructures. Polyelectrolytes, like poly(2-vinyl *N*-methylpyridinium iodide), have also been used to assist the linear assembly of Fe₃O₄ nanoparticles (10–12 nm).⁴⁰ In this attempt, an electrostatic interaction between the magnetic nanoparticles and the positively charged polyelectrolyte firmly fixed the polyelectrolyte macromolecules on the nanoparticles in a linear fashion.

Compared with homopolymers, block copolymers represent a tailor-made surfactant and crosslinker for the synthesis and assembly of magnetic nanoparticles. The block copolymer can be specially designed to satisfy different requirements in a single task: one block as a stabilizing head and another block to lock the conjugated structure of nanoparticles by chemical crosslinking. In the case of Co nanoparticles, it involved the coating of Co nanoparticles with diblock copolymers and the cross-linking of the anchoring layer of the coating copolymer to yield covalently immobilized polymer-coated Co nanoparticle chains (Fig. 14).⁴¹ More specifically, the Co nanoparticles were prepared at high temperature utilizing a diblock copolymer poly(2-cinnamoyloxyethyl methacrylate)-*b*-poly(acrylic acid) (PCEMA-*b*-PAA) as a block-type macromolecular surfactant. The resultant nanoparticles were coated by PCEMA-*b*-PAA with the PAA block directly anchoring on the nanoparticle surface and the PCEMA block stabilizing the nanoparticles in solution. Due to the magnetic dipole–dipole interaction, the Co nanoparticles aggregated into linear chains spaced by PCEMA-*b*-PAA. To build a fully protecting layer for the dipolar chains, they were mixed in a solvent with a second diblock copolymer *Pt*BA-*b*-PCEMA. To the solution was then added methanol, a block selective solvent for *Pt*BA. Above a sufficiently high methanol content, the PCEMA blocks of PCEMA-*b*-PAA and *Pt*BA-*b*-PCEMA collapsed from the solvent phase and the coated dipolar chains were

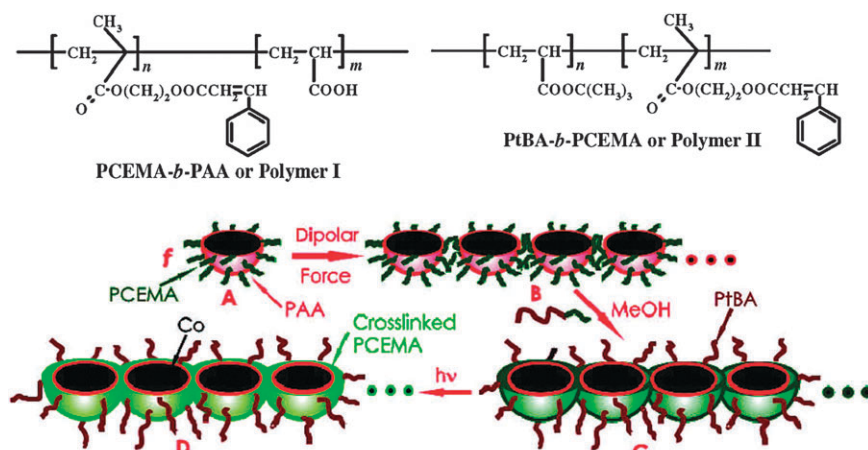


Fig. 14 Cross-sectional schematic for formation (A → B), coating (B → C), and structural locking (C → D) of a Co dipolar chain assisted by block copolymers.⁴¹ Reprinted with the permission of ACS.

rendered colloidally stable by the *Pt*BA chains. Photolysis of such a mixture with UV light led to the cross-linking of the collapsed PCEMA middle layer. This eventually locked the dipolar chains chemically. It is worth mentioning that chemical bonding by sol–gel chemistry to fix the 1D magnetic chains of nanoparticles has also been reported.⁴²

3. Properties and functions

1D magnetic inorganic–organic hybrids possess the general properties and functions of magnetic (nano)materials, as well as the charming feature characters that are derived from a judicious combination of the magnetic response of the magnetic species, the properties donated by the organic phase, and the anisotropic nature of 1D geometry. Compared with their inorganic counterpart, the hybridized state provides task-specific multiple functions, thus broadening the overall application spectrum.

Currently, the organization and manipulation of 1D nanostructures remains a huge challenge in the field of nanomaterials, as further scientific and technological advances in the application of 1D nanostructures in functional nanodevices rely more and more on the ability to assemble them into controllable, ordered, or complex architectures. The collective behavior and interparticle coupling in well-organized 1D nanostructures is of special interest since it may offer new functions or significant improvement of their optoelectronic performance. Among several techniques, magnetic manipulation represents a simple and straightforward method that can be performed independent of the medium. This is for many cases the primary motivation to bring magnetic species into 1D nanomaterials. The fraction of the magnetic component can be as low as less than 1% without impairing the manipulative function. For example, a magnetic electrospinning (MES) method was reported to be able to fabricate well-aligned arrays and multilayer grids of fibers.⁴³ It dealt with the electrospinning of a polymer solution blended with magnetic nanoparticles in a magnetic field. In MES, the polymer solution was magnetized by the addition of a tiny amount (as low as 0.5 wt%) of magnetic nanoparticles. The mixture solution was electrospun into fibers in the presence of a magnetic field generated by two parallel permanent magnets. The magnetic field stretched the fibers across the gap to form a parallel array as they landed on the magnets. The length of the gap between the magnets could be varied from several millimetres to several centimetres, which determined the width of the resultant arrays. Well-organized patterns from double- or multilayers of parallel hybrid nanofibers were easily accessible *via* placing the substrate at different angles in different runs. The resultant nanofibrous arrays could be transferred onto any substrate from any angles with full retention of their structures. This simple and low-cost technique is very useful to organize polymer fibers of a specific function or performance, for example, photoactive PPV fibers. Wang *et al.* reported the fabrication and photoconductive properties of well-aligned PPV/Fe₃O₄ hybrid nanofibers (Fig. 15) by employing two parallel magnets as collector.⁴⁴ After thermal treatment, the magnetic fibers with a diameter in the range of 200–700 nm emitted green fluorescence.

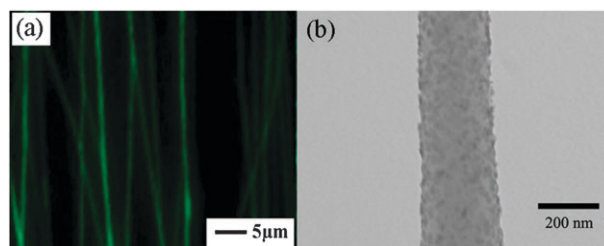


Fig. 15 (a) Fluorescence microscopy image of the PPV/Fe₃O₄ hybrid magnetic nanofiber array prepared by using two parallel magnets as a collector in electrospinning; (b) TEM image of a single nanofiber.⁴⁴ Reprinted with the permission of AIP.

Photoconductor devices fabricated from the PPV/Fe₃O₄ nanofiber array showed high light sensitivity with an $I_{\text{light}}/I_{\text{dark}}$ ratio of 30, good response speed, wavelength sensitivity, and reproducibility.

The addition of the ferromagnetic nickel segment to Au–PPy–Ni–Au multisegmented nanowires allows them to act like tiny magnets that not only interact with an external magnetic field but also with one another and ferromagnetic electrodes. The imposed magnetic field aligned the nanowires in solution parallel to the magnetic field due to the substantially stronger shape anisotropy of the nickel segment, magnetizing the nickel along its cylindrical axis or magnetic easy axis. In the presence of an external magnetic field, the ferromagnetic electrodes magnetized and behaved as micro-magnets, creating strong local fields at the edge of the electrodes where magnetic poles were formed (Fig. 16). These localized magnetic fields dominated nanowire–nanowire dipole interactions for preferential nanowire alignment adjacent to the ferromagnetic electrode. Although, electrode pairs with a single ferromagnetic electrode (the other was gold) did not always facilitate bridging of both the Ni and PPy segments, matching pairs of ferromagnetic electrodes

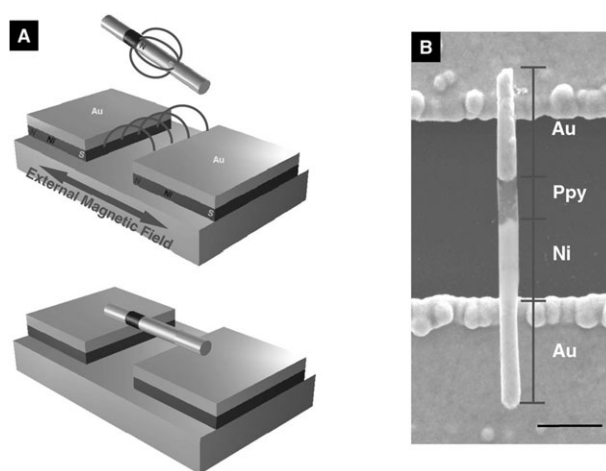


Fig. 16 (A) Schematic illustration of the magnetic assembly of multisegmented nanowires. The lines represent the magnetic field of the nanowire and the ferromagnetic electrodes. Bottom figure showing the placement of different segments of the nanowire on the contact electrodes. (B) SEM image of a single nanowire assembled on prefabricated electrodes (scale bar \approx 1 μ m).⁵ Reprinted with the permission of Wiley-VCH.

dramatically improved the yield. The observation was attributed to both the difference in magnetic fields and the magnetic properties of the Ni segment's neighboring materials. For a single ferromagnetic electrode the magnetic field is strongest at a single edge allowing it to extend further with either end of the Ni segment next to the electrode. However for two ferromagnetic electrodes the magnetic field was focused between two edges and the paramagnetic PPy segment had a lower resistance in this gap than the diamagnetic gold segment. These magnetic interactions between the ferromagnetic electrodes and nanowire segments dictated the placement of the nanowires where the nickel segment was right next to one of the electrodes with the PPy segment bridging the gap, and terminal gold segments overlapping the electrodes to provide better electrical contact. The resulting assemblage demonstrated precise control over alignment of multisegmented nanowires on prefabricated electrodes for single nanowire devices and suggested the potential for an array of high density nanowires with appropriately selected electrode geometry.

In a strong acidic aqueous solution, magnetic components, such as magnetite, can be dissolved, forfeiting its magnetic response. 1D magnetic hybrid nanomaterials can take this advantage to realize the alignment of nonmagnetic 1D objects. A facile and unique process named magnetization–alignment–demagnetization (“MAD”) has been reported to align Te nanorods on a solid substrate. Te is a diamagnetic material, and the direct alignment in a magnetic field is unrealistic. This task can be fulfilled by converting Te nanorods into Te/polymer/magnetite hybrid nanocylinders (Fig. 17). In this process, the Te nanorods were coated with a poly(*tert*-butyl methacrylate) (PtBMA) thin layer on the surface during the preparation. This enabled the nanorods to be well-dispersed in organic solutions. In the following step, oleic

acid-coated magnetite nanoparticles ($d \approx 10$ nm) were attached onto the nanorod surface *via* interaction between polymers and surfactants on their surfaces. Alignment of the as-synthesized nanocylinders on a solid substrate was easily performed by dropping their solution on a substrate and drying in a magnetic field of 0.3 T. Due to the magnetic nanoparticles on the surface, the longitudinal axis (easy axis) of most Te nanorods was parallel to the magnetic field. To recover Te nanorods, a selective etching process in an aqueous HCl solution was carried out to dissolve the magnetite nanoparticles from the nanorod surface. It kept the Te nanorods in an aligned state, as the hydrophobic polymer shell on the nanorod in the aqueous solution acted as a cage, fixing the nanorods on the substrate. After the etching process, the longitudinal axis of these nanorods pointed exclusively to the same direction as the external magnetic field. This methodology by employing 1D magnetic hybrids as intermediates can be broadened as a general method to align nonmagnetic 1D nanostructures in the presence of an external magnetic field.

Superparamagnetic nanoparticles of less than 50 nm have been intensively studied as potential contrast agents for MRI. MRI contrast agents act to improve image quality by reducing the relaxation times and hence altering the nuclear magnetic resonance signal intensity of the water in body tissues containing the agent. Efforts to increase MRI sensitivity have focused on development of new magnetic materials, or improvements in nanoparticle size or clustering. A chain structure of iron oxide nanoparticles with a protective biopolymer layer has been reported to improve the ability of the nanoparticles to circulate, target, and image tumors.^{45,46} Gun'ko *et al.* synthesized linear, chain-like assemblies of iron oxide magnetic nanoparticles which were stabilized and crosslinked by a polyelectrolyte of poly(sodium-4-styrenesulfonate) in

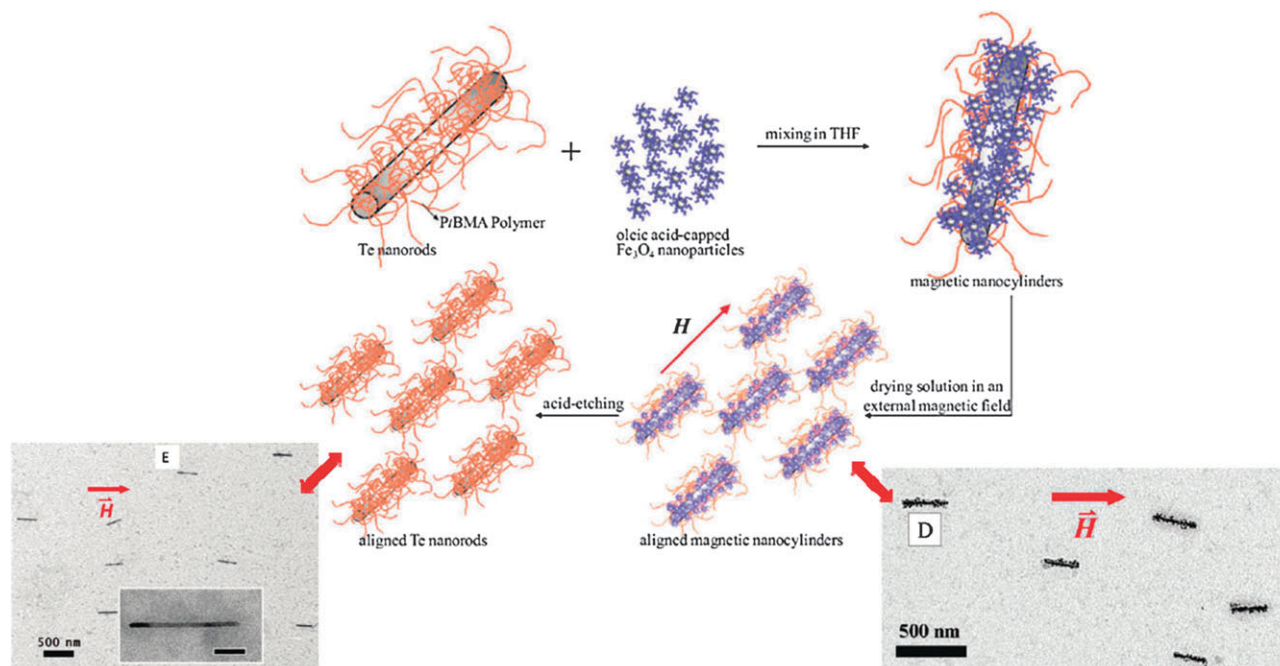


Fig. 17 Illustration of the alignment of Te nanorods *via* a “MAD” process assisted by an external magnetic field.²⁵ Reprinted with the permission of ACS.

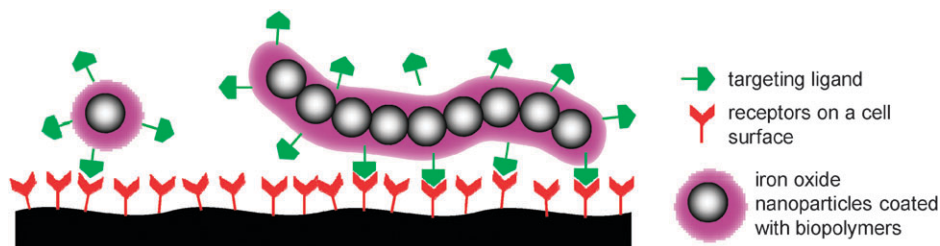


Fig. 18 Conceptual scheme illustrating the increased multivalent interactions between receptors on a cell surface and targeting ligands on a magnetic chain compared with a nanoparticle.⁴⁶ Reprinted with the permission of Wiley-VCH.

the presence of an external magnetic field. After injection of the magnetic fluids of these hybrid 1D magnetic nanostructures in the tail vein of rats, the contrast agent was very quickly cleared from the brain area. It was believed that chain- or worm-like assemblies of magnetic nanoparticles facilitated their easy passage through the circulatory system. In a related biomedicine application, Sailor *et al.* prepared wormlike iron oxide assemblies, which were surface-passivated and firmly fixed by high-molecular weight dextran. They showed improved efficacy both *in vitro* and *in vivo* by enhancing their magnetic relaxivity in MRI, increasing their ability to attach to tumor cells *in vitro*. Compared with a single nanoparticle, the magnetic nanoworm possessed much more targeting ligands on its surface (Fig. 18), although their circulation times were close to each other. Accordingly, the enhanced multivalent interactions between peptide-modified nanoworms and cell receptors amplified their passive accumulation *in vivo* over spherical nanoparticle controls.

In another bio-related application, Greiner *et al.* demonstrated the possibility of controlled movement of hybrid magnetic electrospun fibers to interconnect hippocampal neurons.²⁸ To prepare the fibers, a solution of a fluorescent copolymer of poly(methylmethacrylate-*co*-9-vinylanthracene) (P(MMA-*co*-VA)) with dispersed superparamagnetic Co nanoparticles was electrospun on a rotating drum to afford fibers with a diameter in the range of 1–3 μm . The incorporation of poly(9-vinylanthracene) into fibers allowed for the convenient monitoring of the fibers *via* fluorescence microscopy. The hybrid fibers were further cut into rods of an average length of around 50–100 μm , a dimension scale that was easy to organize and image in a fluorescence microscope. They were dispersed in water and placed on a microscope slide furnished with the fixed embryonic hippocampal neurons grown on coverslips. Manipulation of the fibers was performed by a ferromagnet below the microscope slide. The sequence of fluorescent microscope images (Fig. 19) illustrated the controlled manual motion of the cut electrospun fibers by precise positioning of the fibers between neurons. Apart from a single fiber, several fibers could be moved simultaneously in the same direction, which could be advantageous for multifold simultaneous bridging of the target objects.

The magnetotransport of hybrid chains of CoFe_2O_4 nanoparticles on DNA has been studied by Ivanisevic *et al.* The hybrids were prepared by a combination of chemical synthesis to produce nanoparticles of 5 nm in diameter and molecular templating using DNA to arrange the nanoparticles into

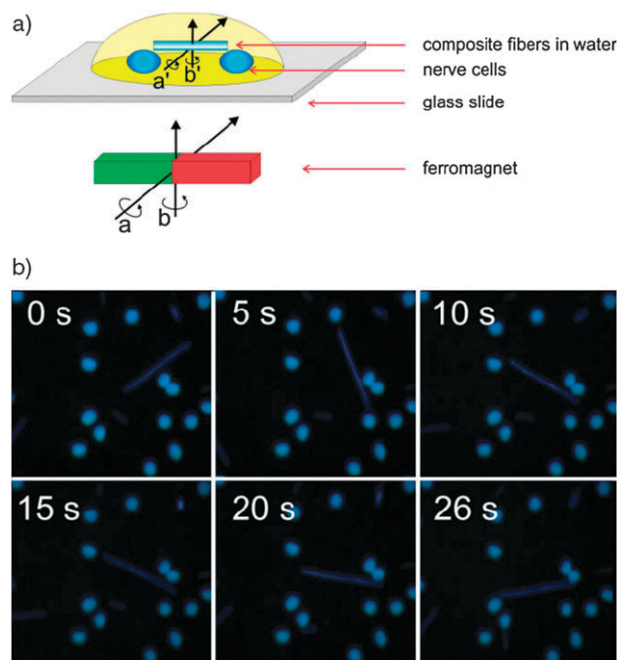


Fig. 19 (a) Schematic image of ferromagnet-assisted movement of electrospun cut Co/P(MMA-co-VA) rod-like fibers, (b) sequence of fluorescence microscope images (frame width: 2.5 μm) captured from a video at different stages of movement of a magnetic hybrid fiber dispersed in a water droplet on a glass slide with stained nuclei of hippocampal cells (blue spots) manipulated manually by a ferromagnet. Reprinted with the permission of Wiley-VCH.

chains. The hybrids displayed significant changes in behavior when external fields were applied. In the transport studies, the sample showed an increasing conductivity in the presence of an increasing external field at 300 K (Fig. 20). When no external or negative fields were applied, the resistance of the sample was an order of magnitude larger than that observed at 20 kOe. The room-temperature magnetoresistance in the CoFe_2O_4 samples reached 82.3% at high fields. The likely mechanism of the magnetoresistance effect observed arose from magnetostatic dipolar interactions. As the nanoparticles were confined into a 1D array, the long-range interactions between the nanoparticles produced coinciding transitions of their magnetic moments. Charge transport in these systems appeared to be dominated by a tunneling mechanism, in which electrostatic charging also played a role. The density of the nanoparticles on the DNA backbone and magnetostatic interactions both caused the conductivity of these nanoparticle

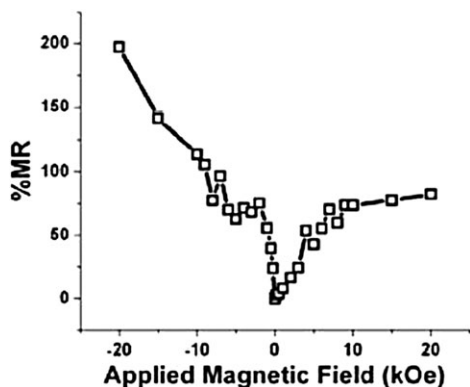


Fig. 20 The magnetotransport response to the field applied along the intrinsic easy axis of the CoFe_2O_4 -nanoparticle-coated DNA (MR: magnetoresistance).³⁵ Reprinted with the permission of ACS.

chains to be increased in an applied field of enough strength to saturate the particles.

Some other properties and functions of 1D hybrid magnetic nanomaterials have been demonstrated by several research groups. For instance, magnetic polypeptide nanotubes prepared by the LbL assembly within polycarbonate membranes have been successfully used as DNA carriers;³ magnetite–PAN nanofibers prepared by electrospinning presented higher coercivity due to decreased interparticle dipolar interaction.²⁹ A small area of $1\text{ cm} \times 1\text{ cm}$ networks of Co–DNA hybrid nanowires showed 50% adsorption of electromagnetic wave, indicating they could be suitable for the electromagnetic wave absorption materials.⁴⁷

4. Concluding remarks and perspectives

This work presents a brief review of the progress in a special family of 1D hybrid nanomaterials which contain magnetic and organic components. We stress the materials synthesis, detailing the state-of-the-art approaches of template-directed synthesis, the electrospinning technique and the conjugation of building blocks. Conceptually, the template route is rather simple and straightforward, provided the template is easy to access. Compared to the other two strategies, it remains at present the major approach in the preparation of 1D hybrid magnetic nanomaterials, not only as a result of a rather large amount of available templates existing in various forms, but also because many physical and chemical treatments or manipulations can be involved in the fabrication process. The unique advantage of the electrospinning technique employed to prepare 1D hybrid magnetic nanomaterials lies in the fact that this processing technique can provide in principle ultralong and continuous hybrid nanofibers. They are important candidates for the study of strong anisotropic effects and properties that are caused and amplified by a high aspect ratio.²⁷ However, as limited by the instrumental setup, not all types of morphologies (Fig. 1) are accessible by this technique in spite that recent advance in the instrumental design have already realized a couple of hierarchical nanostructures. The approach based on the conjugation of magnetic building blocks requires special attention in the choice of building blocks (chemical nature, particles size,

surface properties, *etc.*), the alignment procedure and the fixation mechanism and chemistry applied to the aligned assemblies. Moreover, although the diameter of the formed 1D magnetic hybrids is adjustable by that of nanoparticles chosen, the length is in fact uncontrolled. From a synthetic chemist's perspective, it is extremely encouraging to see that the development of new 1D magnetic hybrid materials with novel morphologies and functions stands well alongside progress in other related fields, such as hybrid nanomaterials, other 1D inorganic nanomaterials,^{48,49} polymer science and chemistry, and device engineering. All these efforts have further pushed the limit of materials design of 1D nanomaterials to a level beyond the predictable expectation. Despite the rapid ongoing progress, a number of challenges and avenues of exploration remain.

According to our point of view, the following directions deserve to be paid special attention to: (1) precise control of the distribution of the magnetic phase. The size, shape, density and distance of the particles are the determining parameters of the performance and functions of the magnetic phase. Controlling all of these structural parameters is apparently a huge challenge and has been realized only occasionally. (2) As a consequence of the magnetic manipulation, 1D magnetic hybrids as a result of the anisotropic shape create ordered patterns on a solid substrate; however, the study of magnetic field-dependent solution properties, such as lyotropic phases or viscosity, has been significantly retarded because of the lack of experimental samples that are colloidally stable at a sufficiently high concentration. Potentially this requires the incorporation of a dense, thick and charged (bio)polymer layer on the surface to afford satisfactory stabilization and repulsion against the gravity and magnetic attractive interactions among individual objects. The intensive research on magnetic nanofluids so far has been chiefly confined to spherical colloids, since they are much easier to produce and stabilize in solution up to a high concentration. Bringing 1D hybrid magnetic nanostructures into solution to form stable magnetic fluids may give rise to a new research branch of magnetic materials. (3) Theoretical modeling, calculation and prediction of these nanostructures, their collective behavior and mutual interaction, have received little attention, which according to our opinion will potentially impair the rapid process in this field. There have been so far only few publications dealing with the interpretation and theory background behind the observed phenomena of 1D hybrid or inorganic magnetic nanomaterials or their assemblies. For example, in a model system of carbon nanotubes filled with magnetite nanoparticles, the average magnetic moment of the magnetic carbon nanotubes has been calculated; they easily formed chain-like assembly in the presence of an external magnetic field due to dipole–dipole interaction, which was supported by the fact that the calculated minimum energy of two needle-like magnets corresponding to their parallel orientation is estimated to be much greater than the energy of thermal excitations.⁵⁰ Meyer *et al.* prepared nickel nanowires that were functionalized with luminescent porphyrins; the dynamics for chain formation have been quantitatively modeled.⁵¹ To understand the self-organization of magnetic nanocrystals in an applied external field, Richardi *et al.* performed Monte Carlo simulations of

Stockmayer fluids confined between two parallel walls.⁵² Apart from providing a deep insight into the mechanism and driving forces of several magnetic phenomena, these efforts enable a quantitative analysis of the magnetic properties.

Acknowledgements

The authors' work was supported by the Deutsche Forschungsgemeinschaft (DFG) within SFB 481 and SPP 1165.

References

- 1 D. L. Leslie-Pelecky and R. D. Rieke, *Chem. Mater.*, 1996, **8**, 1770.
- 2 J. M. Lorcy, F. Massuyeau, P. Moreau, O. Chauvet, E. Faulques, J. Wery and J. L. Duvail, *Nanotechnology*, 2009, **20**, 405601.
- 3 Q. He, Y. Tian, Y. Cui, H. Möhwald and J. Li, *J. Mater. Chem.*, 2008, **18**, 748.
- 4 S. Park, J.-H. Lim, S.-W. Chung and C. A. Mirkin, *Science*, 2004, **303**, 348.
- 5 M. A. Bangar, C. M. Hangarter, B. Yoo, Y. Rheem, W. Chen, A. Mulchandani and N. V. Myung, *Electroanalysis*, 2009, **21**, 61.
- 6 J. Martin and C. Mijangos, *Langmuir*, 2009, **25**, 1181.
- 7 X. Yan, G. Liu, F. Liu, B. Z. Tang, H. Peng, A. B. Pakhomov and C. Y. Wong, *Angew. Chem., Int. Ed.*, 2001, **40**, 3593.
- 8 X. Yan, G. Liu, M. Haeussler and B. Z. Tang, *Chem. Mater.*, 2005, **17**, 6053.
- 9 H. Wang, A. J. Patil, K. Liu, S. Petrov, S. Mann, M. A. Winnik and I. Manners, *Adv. Mater.*, 2009, **21**, 1805.
- 10 M. Zhang, C. Estournes, W. Bietsch and A. H. E. Müller, *Adv. Funct. Mater.*, 2004, **14**, 871.
- 11 Y. Xu, J. Yuan, B. Fang, M. Drechsler, M. Müllner, S. Bolisetty, M. Ballauff and A. H. E. Müller, *Adv. Funct. Mater.*, 2010, **20**, 4182.
- 12 M. T. Klem, M. Young and T. Douglas, *Mater. Today*, 2005, **8**, 28.
- 13 E. T. Simpson, T. Kasama, M. Posfai, P. R. Buseck, R. J. Harrison and R. E. Dunin-Borkowski, *J. Phys. Conf. Ser.*, 2005, **17**, 108.
- 14 R. E. Dunin-Borkowski, M. R. McCartney, R. B. Frankel, D. A. Bazylinski, M. Posfai and P. R. Buseck, *Science*, 1998, **282**, 1868.
- 15 D. Nyamjav, J. M. Kinsella and A. Ivanisevic, *Appl. Phys. Lett.*, 2005, **86**, 093107.
- 16 J. M. Kinsella and A. Ivanisevic, *J. Am. Chem. Soc.*, 2005, **127**, 3276.
- 17 Q. Gu and D. T. Haynie, *Mater. Lett.*, 2008, **62**, 3047.
- 18 Q. Gu, C. Cheng and D. T. Haynie, *Nanotechnology*, 2005, **16**, 1358.
- 19 W. Shenton, T. Douglas, M. Young, G. Stubbs and S. Mann, *Adv. Mater.*, 1999, **11**, 253.
- 20 K. T. Nam, D.-W. Kim, P. J. Yoo, C.-Y. Chiang, N. Meethong, P. T. Hammond, Y.-M. Chiang and A. M. Belcher, *Science*, 2006, **312**, 885.
- 21 M. Kobayashi, M. Seki, H. Tabata, Y. Watanabe and I. Yamashita, *Nano Lett.*, 2010, **10**, 773.
- 22 K. S. Mayya, D. I. Gittins, A. M. Dibaj and F. Caruso, *Nano Lett.*, 2001, **1**, 727.
- 23 M. A. Correa-Duarte, M. Grzelczak, V. Salgueirino-Maceira, M. Giersig, L. M. Liz-Marzan, M. Farle, K. Sieradzki and R. Diaz, *J. Phys. Chem. B*, 2005, **109**, 19060.
- 24 J. Yuan, H. Schmalz, Y. Xu, N. Miyajima, M. Drechsler, M. W. Möller, F. Schacher and A. H. E. Müller, *Adv. Mater.*, 2008, **20**, 947.
- 25 J. Yuan, H. Gao, F. Schacher, Y. Xu, R. Richter, W. Tremel and A. H. E. Müller, *ACS Nano*, 2009, **3**, 1441.
- 26 R. Faridi-Majidi and N. Sharifi-Sanjani, *J. Appl. Polym. Sci.*, 2007, **105**, 1351.
- 27 M. Graeser, M. Bognitzki, W. Massa, C. Pietzonka, A. Greiner and J. H. Wendorff, *Adv. Mater.*, 2007, **19**, 4244.
- 28 O. Kriha, M. Becker, M. Lehmann, D. Kriha, J. Krieglstein, M. Yosef, S. Schlecht, R. B. Wehrspohn, J. H. Wendorff and A. Greiner, *Adv. Mater.*, 2007, **19**, 2483.
- 29 D. Zhang, A. B. Karki, D. Rutman, D. P. Young, A. Wang, D. Cocks, T. H. Ho and Z. Guo, *Polymer*, 2009, **50**, 4189.
- 30 T. Placido, R. Comparelli, F. Giannici, P. D. Cozzoli, G. Capitani, M. Striccoli, A. Agostiano and M. L. Curri, *Chem. Mater.*, 2009, **21**, 4192.
- 31 S. Xiao, M. Shen, R. Guo, S. Wang and X. Shi, *J. Phys. Chem. C*, 2009, **113**, 18062.
- 32 V. Kalra, J. Lee, J. H. Lee, S. G. Lee, M. Marquez, U. Wiesner and Y. L. Joo, *Small*, 2008, **4**, 2067.
- 33 T. Song, Y. Z. Zhang and T. J. Zhou, *J. Magn. Magn. Mater.*, 2006, **303**, e286.
- 34 A. O. Adeyeye and M. E. Welland, *Appl. Phys. Lett.*, 2002, **80**, 2344.
- 35 J. M. Kinsella and A. Ivanisevic, *J. Phys. Chem. C*, 2008, **112**, 3191.
- 36 B. D. Korth, P. Keng, I. Shim, S. E. Bowles, C. Tang, T. Kowalewski, K. W. Nebesny and J. Pyun, *J. Am. Chem. Soc.*, 2006, **128**, 6562.
- 37 B. Y. Kim, I.-B. Shim, Z. O. Araci, S. S. Saavedra, O. L. A. Monti, N. R. Armstrong, R. Sahoo, D. N. Srivastava and J. Pyun, *J. Am. Chem. Soc.*, 2010, **132**, 3234.
- 38 P. Y. Keng, B. Y. Kim, I.-B. Shim, R. Sahoo, P. E. Veneman, N. R. Armstrong, H. Yoo, J. E. Pemberton, M. M. Bull, J. J. Griebel, E. L. Ratcliff, K. G. Nebesny and J. Pyun, *ACS Nano*, 2009, **3**, 3143.
- 39 Y. Xiong, Q. Chen, N. Tao, J. Ye, Y. Tang, J. Feng and X. Gu, *Nanotechnology*, 2007, **18**, 345301.
- 40 R. Sheparovych, Y. Sahoo, M. Motornov, S. Wang, H. Luo, P. N. Prasad, I. Sokolov and S. Minko, *Chem. Mater.*, 2006, **18**, 591.
- 41 Z. Zhou, G. Liu and D. Han, *ACS Nano*, 2009, **3**, 165.
- 42 H. Singh, P. E. Laibinis and T. A. Hatton, *Langmuir*, 2005, **21**, 11500.
- 43 D. Yang, B. Lu, Y. Zhao and X. Jiang, *Adv. Mater.*, 2007, **19**, 3702.
- 44 Y. Xin, Z. H. Huang, L. Peng and D. J. Wang, *J. Appl. Phys.*, 2009, **105**, 086106.
- 45 S. A. Corr, S. J. Byrne, R. Tekoriute, C. J. Meledandri, D. F. Brougham, M. Lynch, C. Kerskens, L. O'Dwyer and Y. K. Gun'ko, *J. Am. Chem. Soc.*, 2008, **130**, 4214.
- 46 J.-H. Park, G. von Maltzahn, L. Zhang, M. P. Schwartz, E. Ruoslahti, S. N. Bhatia and M. J. Sailor, *Adv. Mater.*, 2008, **20**, 1630.
- 47 C.-H. Lin, S.-Y. Tong, S.-W. Lin, H.-L. Chen, Y.-C. Liu, H.-K. Lin, W.-L. Liu, S.-Y. Cheng and Y.-H. Wang, *Mater. Res. Soc. Symp. Proc.*, 2006, **921E**.
- 48 J. Yuan and A. H. E. Müller, *Polymer*, 2010, **51**, 4015.
- 49 Y. Xia, P. Yang, Y. Sun, Y. Wu, B. Mayers, B. Gates, Y. Yin, F. Kim and H. Yan, *Adv. Mater.*, 2003, **15**, 353.
- 50 G. Korneva, H. Ye, Y. Gogotsi, D. Halverson, G. Friedman, J.-C. Bradley and K. G. Kornev, *Nano Lett.*, 2005, **5**, 879.
- 51 M. Tanase, L. A. Bauer, A. Hultgren, D. M. Silevitch, L. Sun, D. H. Reich, P. C. Searson and G. J. Meyer, *Nano Lett.*, 2001, **1**, 155.
- 52 J. Richardi, M. P. Pileni and J. J. Weis, *Phys. Rev. E*, 2008, **77**, 061510.